analytical chemistry

Article

pubs.acs.org/ac

# Hand-Held Reader for Colorimetric Sensor Arrays

Jon R. Askim and Kenneth S. Suslick*

Department of Chemistry, University of Illinois at Urbana−Champaign, 600 South Mathews Avenue, Urbana, Illinois 61801, United States

Supporting Information

**ABSTRACT:** An inexpensive hand-held device for analysis of colorimetric sensor arrays (CSAs) has been developed. The device makes use of a contact image sensor (CIS), technology commonly used in business card scanners, to rapidly collect low-noise colorimetric data for chemical sensing. The lack of moving parts and insensitivity to vibration allow for lower noise and improved scan rates compared to other digital imaging techniques (e.g., digital cameras, flatbed scanners); signal-to-noise ratios are a factor of 3−10 higher than currently used methods, and scan rates are up to 250 times faster without compromising sensitivity. The device is capable of real-time chemical analysis at scan rates up to 48 Hz.


Development of rapid, sensitive, portable, and inexpensive systems for identification of gaseous analytes has become an urgent societal need and has important applications ranging from the chemical workplace, to security screening, to even health monitoring of the general population. The use of colorimetric sensor arrays has proven to be a fast, sensitive, and versatile method of liquid, vapor, and gas analysis where the specificity derives from the pattern of response from cross-reactive sensor arrays rather than individual sensors for specific analytes.[1−5] Colorimetric sensor arrays have been successfully used to differentiate among diverse families of analytes, ranging from toxic industrial chemicals,[6−9] to various foods and beverages,[10−17] to pathogenic bacteria and fungi.[18−23] Unfortunately, these methods have generally been limited to use in laboratory settings due to the fragility and bulk of the instrumentation.

The use of colorimetric sensor arrays would benefit greatly from a portable, low-noise optical reader with onboard processing capability. To that end, we have developed a hand-held reader to analyze colorimetric sensor arrays that is a self-contained, truly portable analytical device. The hand-held reader uses a color contact image sensor (CIS) that contains a linear CMOS (complementary metal-oxide semiconductor) sensor array for optical transduction;[24,25] due to their short focal distances, CIS devices are commonly used as business card scanners and in some flatbed scanners. The hand-held reader also incorporates a disposable sealed cartridge, a diaphragm micropump for analyte flow control, and onboard electronics that provide rapid, low-noise measurement of red, green, and blue reflectivity of a linearly arranged colorimetric sensor array during exposure to gaseous analytes. The hand-held reader is also capable of performing statistical evaluation (e.g., classification) in real time.

## EXPERIMENTAL SECTION

**Hand-Held Reader Construction.** M116 CIS modules were purchased from CMOS Sensor Inc. (Mountain View, CA, U.S.A.).[25] Diaphragm micropumps were purchased from Schwarzer Precision (Essen, NRW, Germany).[26] Onboard processing and device operation were controlled using custom-designed electronics (D3 Engineering, Rochester, NY, U.S.A.) centered around a TMS320DM6437 digital signal processor as the CPU (Texas Instruments, Dallas, TX, U.S.A.). Other components (chassis, flow manifolds, etc.) were custom-designed (iSense Systems/Metabolomx, Mountain View, CA, U.S.A. and Intelligent Product Solutions, Hauppage, NY, U.S.A.). The component costs of the hand-held reader are modest: M116 CIS module ($80, CMOS Sensor Inc.), NHD-042H1Z LCD screen ($18, Newhaven Display), two-position membrane switch ($10, SSI Electronics), and SP-100-EC-LC diaphragm micropump ($80, Schwarzer Precision). Prototype components consisted of the digital processor and chassis; we estimate that the digital processor could be replaced with commercially available components for <$100 and a plastic chassis could be mass-produced for <$10.

**Colorimetric Sensor Array Cartridge.** A custom linear cartridge was designed to fit the hand-held reader and provide a narrow flow path for analyte exposure of a colorimetric sensor array. Polypropylene membranes (0.2 μm) were used as printing substrates for the array and were purchased from Sterlitech Corporation (Kent, WA, U.S.A.). The polypropylene was mounted to an injection-molded low-volatility white polycarbonate cartridge (Dynamic Plastics, Chesterfield Twp, MI, U.S.A.) using a solvent-weld (dichloromethane).

**Received:** April 21, 2015
**Accepted:** July 6, 2015
**Published:** July 15, 2015





DOI: 10.1021/acs.analchem.5b01499
*Anal. Chem.* 2015, 87, 7810−7816

The colorimetric sensor array then robotically printed on the substrate using procedures described previously.[8] Arrays used for evaluation of the hand-held reader used 28−48 colored spots printed at 1.0 or 1.2 mm center-to-center distances; 1.2 mm spacing provided more consistent physical separation of the sensor elements. All reagents were analytical reagent grade, purchased from Sigma-Aldrich and used without further purification.

After colorimetric sensor arrays were printed, they were thoroughly dried under nitrogen. A glass microscope slide was then snapped into the cartridge, providing a gastight seal against a Viton O-ring, as shown in Figure 1. This provides a nearly ideal flow path for the analyte stream with a flow volume of ∼85 μL. The arrangement of the CIS and the linear colorimetric sensor array is shown in Supporting Information Figure S1.

**Figure 1.** Photographs of the cartridge and a colorimetric sensor array showing side and array views. The sensor array shown here has 40 sensor elements at 1.2 mm center-to-center spacing and represents typical printing quality.

**CIS Calibration.** As designed, the CIS outputs an analog signal between ∼0 and 3.4 V that is fed into a 12-bit analog−digital converter (ADC) with a 5 V reference voltage. Initially, illumination parameters (i.e., LED voltage and pulse widths) were set to their maximum allowed values in order to determine the optimal pixel clock rate; a pixel clock of 500 kHz (1478 total pixels, which gives a 3.0 ms capture window for each of the red, green, and blue LEDs) was found to be ideal for maximizing the signal from a white substrate without significant overexposure. To minimize response variability between pixels and to maximize sensitivity, illumination levels were further optimized by varying the voltage for each of the red, green, and blue LEDs; these optimized illumination levels are a one-time calibration of the CIS and were used for all further experiments with all five instruments constructed. Individual pixels vary slightly in responsivity; pixels (and by extension, separate scanner units) were calibrated by normalizing from data obtained using a cartridge containing a blank polypropylene substrate for a 100% reflectance standard and turning off all illumination for a 0% reflectance standard. These calibration standards are an additional one-time calibration for each individual hand-held reader.

**Array Testing.** All tests were performed using a built-in diaphragm micropump (approximately 580 $cm^3$/min flow rate). For our convenience in laboratory-controlled gas sampling, air was drawn through a bubbler containing deionized water to generate 100% relative humidity (RH) flow for the control gas stream. The analyte gas stream was generated by drawing air through a bubbler containing dilute aqueous ammonia to generate an $NH_3$ gas stream, whose concentration was confirmed by in-line analysis using an FT-IR multigas analyzer, MKS Instruments model 2030; typical concentration was 50 ppm. Strict humidity control is not a requirement for use of these colorimetric sensor arrays, whose insensitivity to changes in humidity have already been well-established.[6,8,9,27−32] Control and analyte gas streams were pulled through the cartridges with the onboard micropump and scanned at 1.0 Hz. The optical components are isolated from the cartridge, so the optics are not exposed to analyte vapor or humidity in the analyte stream. The arrays were initially exposed to the control gas line for 10 min before being switched to the analyte line for 10 min; exposure to the control gas eliminates any optical or chemical effects due to large humidity changes upon switching to the analyte gas. The colorimetric sensor array response is sufficient for analysis even after only a few seconds of equilibration and exposure, but the exposure times were intentionally made extremely long (i.e., 10 min) in order to guarantee total equilibration with the analyte gas stream and thus eliminate any potential for change in the sensor array response during the gathering of noise and statistical data using multiple scans over a short period of time.

**Data Processing.** All data processing on the hand-held device was done using custom-designed software. Spot location followed a two-step process: first, the array is initially assumed to have perfectly defined spacing and then those initial position are further refined. Spot locations were initially estimated algorithmically by sweeping over the array in order to locate an appropriate number of adjacent spot centers with a 24-pixel (approximately equal to 1.0 mm) center-to-center distance that gave the highest total deviation from the background color (i.e., this assumes ideal printing of the array) as defined by total sum of the squared Euclidean distance of pixel responses. Due to minor imperfections in printing positions inherent in pin-printing, however, spot distances are not perfectly uniformly spaced; the software thus further refined positions to account for individual variation in the center location of each printed spot by finding the pixel which gave the minimum in spatial

**Table 1. Summary of Parameters Used in Compared Imaging Methods[a]**

| method | sensor type | focal distance | pixel resolution (ppi) | scan rate (Hz) |
|---|---|---|---|---|
| hand-held reader | CIS CMOS | ≈2 mm | 600 | 2.0[b] |
| flatbed scanner | CIS CCD | ≈2 mm | 590 | 0.02 |
| DSLR camera | 2D CMOS | 30 cm | 900 | 30 |
| smartphone | 2D CMOS | 10 cm | 560 | 30 |

[a]Pixel resolution (i.e., pixels per inch, ppi) was calculated using known 1.0 mm reference distances. [b]Scan rates for the hand-held device were chosen to be 2.0 Hz; scan rate is adjustable with an upper limit of 50 Hz.



DOI: 10.1021/acs.analchem.5b01499
*Anal. Chem.* 2015, 87, 7810−7816

variance over a 9-pixel window (i.e., the center of the spot is where the color is most uniform and changes the least over a short distance). To evaluate the effectiveness of this protocol, spot widths were varied manually in order to examine the effect of feature size on resultant signal-to-noise ratio (S/N); 9-pixel minimization proved optimal.

Data processing for two-dimensional (2D) images (DSLR, iPhone, and flatbed scanner) was performed using proprietary spot-finding software designed by iSense, Inc. (Mountain View, CA); using this software, spot centers and sizes are initially set manually, and the software optimizes these spot locations in a batch process after data collection across all images in an individual experimental trial.

**Device Comparison and Characterization.** Four separate imaging devices were compared, and their relevant parameters are described in Table 1: the hand-held reader (which uses a stationary linear CMOS-based CIS), a high-end consumer-grade flatbed scanner (Epson V600, which uses Epson ReadyScan LED technology, i.e., a white LED illumination bar), a high-end consumer-grade DSLR camera (Canon EOS 5D Mark II), and a high-end consumer-grade smartphone (Apple iPhone 5S). The DSLR and smartphone methods required external illumination ("natural white" LED light strips, purchased from SuperBrightLEDs.com, used with a current controlled power supply) and had different nonzero focal distances; the focal distances used were the minimum necessary in order to ensure appropriate illumination of the chemical sensor arrays (e.g., elimination of shadows obscuring sensor elements and elimination of unwanted specular reflection).

Noise statistics for each of these imaging methods were quantified by comparing images taken of a colorimetric sensor array that was equilibrated with the ambient environment (i.e., an unexposed colorimetric sensor array). Images from each device were collected by scanning at least 20 frames of the colorimetric sensor array. The last 10 frames obtained in each experiment were then used to obtain color data; each spot's color values consisted of red, green, and blue (RGB) values which are themselves composed of data averaged from multiple pixels depending on the spot size: i.e., each spot's RGB values resulted in 87 separate values (dimensions) for a 29-spot array. Standard deviations for each dimension were calculated from the 10 scans, and the noise parameter for each imaging methodology was quantified by using the average of these standard deviations among all dimensions.

The edges of any colorimetric sensor spot represent, of course, a discontinuity in the measured RGB values. As a consequence, colors measured near the edges of a spot show increased variability (among sequential scans) when subjected to small variations in center position (i.e., physical jitter) compared to measurements near spot centers. This increased variability is due to changes in the alignment of physical location on the sensor array to specific pixels in the imager from scan to scan and is therefore sensitive to physical motion (jitter). In order to investigate the magnitude and effect of physical jitter in each of these methods, spot center positions were shifted across the image horizontally (i.e., all digital spot centers are shifted simultaneously by $N$ pixels in the $X$ direction, and $N$ is varied) and noise was calculated as a function of this shift by comparison among multiple scans. Two-dimensional methods (smartphone, flatbed scanner, and video camera) used a 4-pixel radius circular spot from the measurement center point (resulting in 13 pixels), while the one-dimensional data obtained from the CIS used a 4-pixel linear spot from the measurement center point (resulting in four pixels). All appropriate gas flow apparatuses were active during these scans (i.e., the diaphragm micropump for the hand-held device and mass flow controllers for the smartphone, flatbed scanner, and video camera). The hand-held reader was further characterized by obtaining the response profiles upon varying illumination intensity.

## RESULTS AND DISCUSSION

Colorimetry initially evolved as a slow, bulky, qualitative analysis method; techniques such as colorimetric titration and spot tests involved multiple milligrams of material and were evaluated with little more than inspection by eye.[33] Improvements in microelectronics have allowed for significant miniaturization of optical transduction components which in turn allows for faster, smaller, quantitative analyses that are evaluated electronically. The imaging methods used to evaluate gas-phase colorimetric sensor arrays involve the use of flatbed scanners,[6,8,9,27,28,30−32,34] digital cameras,[35−42] and smartphone cameras (often with associated analysis software).[43−47] These methods are inexpensive, powerful, and significant improvements over classical qualitative techniques; nonetheless, the use of off-the-shelf hardware leaves much room for additional improvement and optimization. The analyses still generally require manual data processing with a separate device, and the

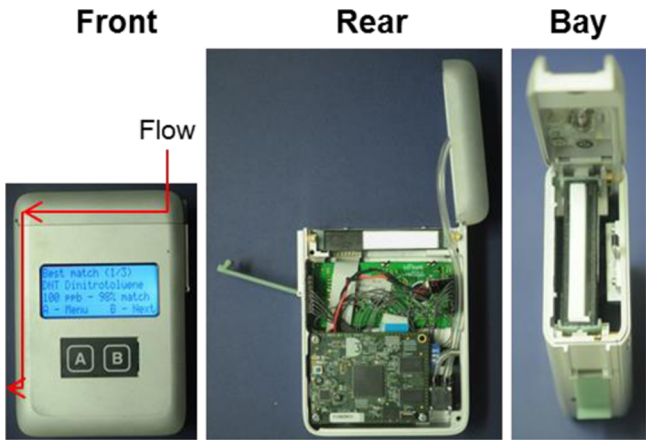


**Figure 2.** Photographs of the hand-held reader including front, rear, and cartridge bay views. Dimensions are 12.5 cm tall by 9.5 cm wide by 4.0 cm thick. The rear panel and 9 V battery were removed in order to provide a better view of the internal electronics and diaphragm micropump (located in rear image, lower right).

**Table 2. Relevant Component Parameters of the Hand-Held Reader**

| | |
|---|---|
| scanner size | 12.8 cm × 9.5 cm × 4.0 cm |
| scanner weight | 460 g + battery + cartridge |
| cartridge size | 7.9 cm × 2.8 cm × 1.0 cm |
| cartridge weight | 11 g |
| battery weight | 48 g |
| static pressure[a] | 550 mbar |
| pump rate[a] | 50−580 $cm^3$/min, adjustable |
| current draw | ∼400 mA at 100% duty |
| battery charge | 1200 mAh |
| scan time | 11 ms |

[a]Ref 26.



DOI: 10.1021/acs.analchem.5b01499
Anal. Chem. 2015, 87, 7810−7816

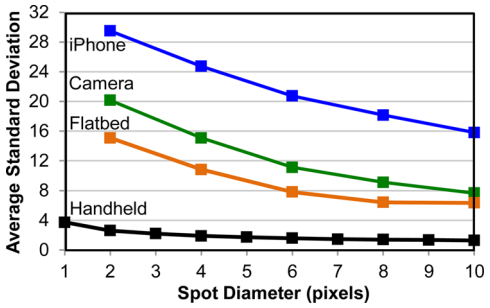


**Figure 3.** Typical noise observed in detected spots as a function of spot size in the hand-held reader, flatbed scanner, DSLR camera, and smartphone camera; standard deviation shown is determined from 10 scans of an array with 29 spots. Note that each of these methods uses 12-bit color space (i.e., [0−4095]) and the dynamic range defined by the difference between fully white and fully black areas is approximately equal for each (i.e., ~2750).

complete apparatuses themselves are also bulky due to the size of both the imaging instrumentation and essential auxiliaries (i.e., gas flow controllers, illumination sources, and external devices required for data processing).

In a similar vein, portable instrumentation for liquid-phase analytes has found some success in urine, saliva, and pH sensing.[18,19,48,49] These methods use only single-point measurements (vs continuous monitoring) and usually require significant operator input, e.g., manual dipstick testing or downloading and manual processing of collected data on a separate computer.

In order to create a portable reader designed for gas-phase analysis with colorimetric sensor arrays, we have developed a hand-held reader. The device is a self-contained, truly portable analytical device with a portable, low-noise optical reader and onboard processing capability.

**Device Construction.** The hand-held reader was designed with a compact form factor in which a CIS optically images the reflectance from a colorimetric sensor array rigidly held ≈2 mm from its surface. The CMOS array present in the CIS is a broadband photodetector; RGB reflectance values are measured by sequentially illuminating the array with red, green, and blue LEDs. A general schematic for operation with a sealed colorimetric sensor array cartridge is shown in the Supporting

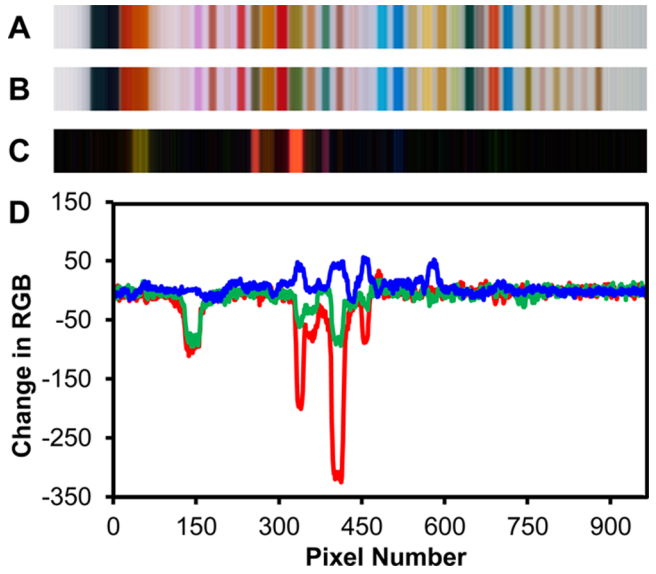


**Figure 5.** Differential array response to $NH_3$ at PEL concentration (50 ppm). (A) Image before exposure. (B) Image after 15 s exposure. (C) Difference image of A and B. (D) Graph of data used to construct C. Images are projected onto 8-bit RGB color space (i.e., [0−255]) for display; images A and B were normalized to a uniform white substrate, while difference image C was normalized to maximum and minimum difference values. Maximum S/N was approximately 280.

Information as Figure S1, light emission profiles are provided as Supporting Information Figure S2, and an illumination timing chart for the CIS is given in Supporting Information Figure S3. Additionally, the chassis itself minimized stray light exposure.

One primary application of colorimetric sensor arrays is monitoring and analysis of gaseous analytes.[1] To accommodate this, a cartridge was designed to fit the hand-held reader and provide a low-volume flow path for analyte exposure of a colorimetric sensor array. The array is printed on a substrate (e.g., polypropylene membrane) and mounted to the cartridge, which is then sealed using a glass microscope slide that sits against a Viton O-ring, as shown in Figure 1. A flow system using a diaphragm micropump was incorporated to allow for gas exposure at ambient pressure without the need for external attachments; the cartridge outflow port was sealed to a gas flow

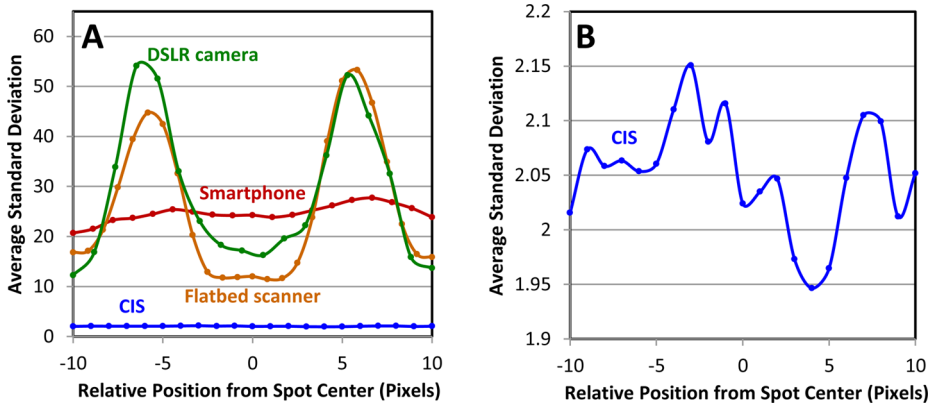


**Figure 4.** Reproducibility of spot imaging as a function of position across the spot, showing the appearance of edge effects. On the *x*-axis, 0 represents the spot center and ±10 represent the space between spots. (A) Comparison of the observed noise from four imaging devices vs distance from the physical center of the dye spots, averaged over all 29 spots. (B) Greatly expanded scale for the standard deviation of the noise measured for imaging using the CIS; no edge artifacts are observed for the CIS. An identical chemical sensor array was used for all scans; relative spot positions were normalized to the resolution of the CIS (600 ppi).



DOI: 10.1021/acs.analchem.5b01499
*Anal. Chem.* 2015, 87, 7810−7816

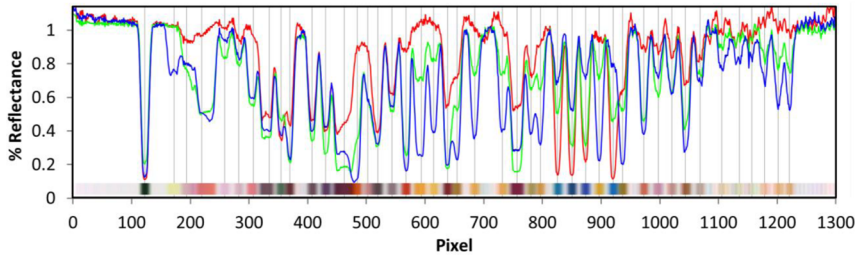


**Figure 6.** Results of spot-finding procedure applied to a problematic colorimetric sensor array. The print quality of this array was deliberately poor in order to test the resilience of the spot-finding algorithm; irregular spacing and overlap among sensor elements were intentional and are not present in typical sensor arrays (cf. Figure 1). Normalized RGB data is shown above an image of the array in red, green, and blue traces. Vertical gray lines correspond to spot centers and show accurate location of 44 of 45 spot locations and all three gaps.

manifold by compression of an O-ring upon closure of the top latch (Figure 2). The micropump can produce a static pressure of ∼500 mbar and was powerful enough to pull vapor analytes through bubblers and loosely packed tubes of silica gel.

Digital data was produced from the analog output of the CIS using a 12-bit ADC. The onboard processor used a 700 MHz CPU to control component behavior and image processing; the internal bus and CPU are capable of transferring images and performing these relatively simple analyses at rates much greater than the 48 Hz scan rate. A database of relevant sensor responses is stored on the hand-held sensor enabling classification in real time. User control for autonomous modes (e.g., real-time monitoring and comparison to known databases) was provided by a simple LCD screen and two-button control scheme. Relevant specifications are shown in Table 2.

**Scan and Processing Rate Comparison.** Previous studies with colorimetric sensors use flatbed scanners[6,8,9,27−32,34] or digital cameras,[35−42] both of which capture a series of large, high-resolution two-dimensional images that are then analyzed using external software. The scan rates of each of these methods are primarily regulated by acquisition and data transfer speeds. In order to make a useful set of comparisons among available imaging devices, we examined an Epson V600 flatbed scanner, an iPhone 5s, a Canon EOS 5D Mark II DSLR camera, and the hand-held reader (which uses a CMOS Sensor Inc. M116 CIS). The Epson V600 flatbed scanner has a moving scanning bar and transfers images directly to the connected computer, which limits its scan rate: 800 dpi images of a typical 2.5 cm × 2.5 cm array take approximately 45 s to acquire and transfer, while higher-resolution images take even longer. DSLR cameras, on the other hand, are not limited by moving parts and have higher bandwidth data transfer methods available; a typical video mode using the DSLR has a collection rate of 30 Hz with a transfer rate of approximately 1−10 Hz during batch transfer, which means that 1 min of video data requires between 3 and 30 min to transfer the data from the camera to a computer for external processing. Smartphones such as the iPhone 5s operate similarly to DSLR cameras but also have onboard processing potential similar to the hand-held reader, and data transfer times can thus be assumed to be zero; in-depth comparison would require access to specific onboard software (i.e., apps) dedicated to scanning similar chemical sensor arrays, so at present only hardware comparisons apply when considering use of a smartphone for array analysis. The hand-held reader described here is capable of scan rates of 48 Hz with essentially real-time processing (i.e., faster than time between subsequent scans) without affecting consistency, as shown in Supporting Information Figure S4.

Images collected with a flatbed scanner or camera are typically processed in batch using a manually calibrated spot finder and can require additional steps (e.g., file conversion, extraction, or image cropping) which significantly increases processing time making real-time analysis impossible. Dedicated software could potentially eliminate these secondary steps, so comparison also requires looking at the fundamental nature of two-dimensional versus one-dimensional images as they apply to colorimetric sensor arrays. During imaging, spot centers move relative to the imaging device and are not perfectly aligned relative to each other; determining the locations of these spots (i.e., spot finding) is the primary bottleneck in data processing. The origin of this problem is twofold: First, due to the realities of printing large numbers of arrays, sensor spot centers are not always perfectly aligned relative to each other. Second, when arrays are positioned for imaging, the spot locations are not aligned identically relative to the imaging device (i.e., pixel positions of sensor elements).

Data handling, and specifically spot finding, with one-dimensional images collected by the hand-held reader is relatively simple and fast compared to handling two-dimensional images: (1) the file size is much smaller (e.g., 1440 pixels compared to 30 × 1440 or more pixels for the same linear array), (2) spot-finding methods are much simpler for one-dimensional data than for two-dimensional data (i.e., there are no rotational or vertical degrees of freedom in one-dimensional data),[2] and (3) the fraction of pixels relevant to image analysis is much greater in one-dimensional images (i.e., data efficiency is improved because pixels corresponding to nonsensor and interstitial areas are minimized).

Combining the improvements in data transfer and increased speed with one-dimensional spot-finding methods, image processing with the hand-held device can be performed continuously in real time. With basic data collection, the primary bottleneck in the hand-held device is actually the exposure time of the CIS itself: spot finding (measured at ∼6 ms) takes approximately half the time of a single scan cycle (measured at ∼11 ms).

**S/N Comparison.** Two-dimensional imaging methods use a number of pixels per sensor element that is proportional to the square of the chosen spot diameter; for the hand-held reader with its linear CIS, the number of pixels is linearly proportional to the spot diameter. One might have expected that the much larger number of pixels per spot in 2D methods would translate to a lower calculated noise simply by virtue of signal averaging. Experimentally, however, this is not the case: as illustrated in Figure 3, the hand-held reader shows lower average noise per spot than other methods for every tested spot size; a typical profile showing the noise of each spot is shown in Supporting


DOI: 10.1021/acs.analchem.5b01499
*Anal. Chem.* 2015, 87, 7810−7816

Information Figure S5. The smallest improvement with the CIS is approximately 5-fold (i.e., compared to the flatbed scanner with large spot size), and the largest improvement is more than 25-fold (i.e., compared to the smartphone with small spot size). The relative change in observed noise as the spot size increases (i.e., the trend as spot size varies) is similar among all four methods tested. It is also worth noting that the difference in observed noise per pixel (rather than per spot) is even larger, as the two-dimensional methods use more pixels per spot (i.e., $\sim\pi r^2$ pixels in 2D methods vs $\sim 2r$ pixels in the hand-held device).

Optical reading of arrays must also deal with the finite size of sensor spots. Printed spots have discontinuities at their edges: each sensor has some more or less uniform colored area at its center whose coloration eventually transitions (either gradually or abruptly) to a blank space between spots or to another overlapping spot. In the presence of physical jitter or vibration, there will be artifacts induced in color difference measurements at the edge of the spots. To maximize the response consistency for each spot, the most uniform area of each spot should be compared before and after exposure; i.e., avoid the edge regions. This minimizes the effect of physical jitter on the digital output. The usable spot radius is thus less than the apparent radius defined only by a printed spot's edge; this is analogous to capturing the top of a plateau and avoiding the cliff at the edge.

The sensitivity of each imaging technique to physical jitter can be measured by observing such edge region artifacts. If one measures the optical response across a spot, small changes in spot position (due to physical jitter) will result in significant apparent color changes at the spot edges, resulting in large standard deviations in color values measured near the edges, as seen in Figure 4. Dramatic increases in noise near the spot edges compared either to the spot center (located at 0 pixels) or to the areas between spots (located at −10 and +10 pixels) are observed in imaging with the flatbed scanner or the video camera. Images taken with an iPhone 5s camera show this edge effect to a lesser extent. Observed noise using the CIS is substantially decreased relative to these other methods and has no apparent correlation with relative position whatsoever (Figure 4B).

Edge artifacts of the sort seen in Figure 4A are explained by physical motion (i.e., jitter) between individual scans, which contributes significantly to the observed noise in imaging methods. In the case of a flatbed scanner, a moving scan bar controlled with servos introduces jitter in the location of the imaged pixels. In the case of the digital camera and the smartphone, the relatively long distance between the colorimetric sensor and the optical lens likely made the methods more susceptible to physical jitter caused by vibration. With the necessary focal lengths for typical camera lenses, it is difficult to maintain absolute structural rigidity and eliminate relative motion. The smartphone focal length is one-third of the DSLR camera (10 vs 30 cm), which contributes to the improvement in noise observed with the smartphone camera; additionally, the imaging software used in a smartphone has many automatic processing features built-in (importantly, including antishake software) and may have had an effect both in terms of the edge−center difference and overall measured noise. For the CIS, the substantial decrease in distance between the optical sensor element relative to spots (≈2 mm) and the absence of any moving components essentially eliminates the artifacts induced by jitter. Importantly for the CIS, adding physical vibration (e.g., turning on the gas micropump) did not have any effect on measured noise values.

**Proof of Concept: Array Analysis.** To show the utility of the device, an array known to be sensitive to toxic industrial chemicals containing acid- and base-treated pH indicators, porphyrins, and other chemoresponsive dyes (described in previous papers[8]) was exposed to a stream of $NH_3$ vapor at roughly its OSHA permissible exposure limit (PEL) of 50 ppm. Digital output from the 12-bit ADC ranged from approximately 50 to 2800 (i.e., ∼2750 possible values, giving approximately 11 bits of color resolution), corresponding to 0% and 100% reflectance, respectively. The maximum output from the CIS was adjusted by limiting the total light intensity so as to avoid loss of sensitivity due to overexposure; this is primarily a function of total reflectivity of the cartridge (specifically its internal flow channel), so adjustment of illumination intensity is a one-time calibration. Results of array exposure after 15 s are shown as Figure 5.

Spot locations were determined automatically by using a spot-finding algorithm. As a test of this algorithm, a 45-spot array with intentionally added gaps and semioverlapping spots was printed at 1.0 mm (approximately 23.6 pixel) spacings (Figure 6). Each spot had a full-width half-maximum of approximately seven pixels, though this was intentionally made somewhat larger for several spots. To determine locations of spots versus space between spots, a simple spot-finding algorithm was used (cf. the Supporting Information for detailed description). This algorithm was tested with an array containing 45 spots and three interspersed gaps (i.e., blank areas not containing any sensor spots), as shown in Figure 6. In order to test the resilience of the algorithm, the print quality of this array is intentionally poor and contains irregular spacing and obvious overlap among some sensor elements. As shown in Figure 6, 44 of 45 printed spots were accurately located, and all three gaps were correctly identified; one spot (fifth from the left in Figure 6) was missed by the algorithm due to its color similarity and physical overlap with the adjacent spot (fourth from left).

With the CIS, the color data has only a single search dimension (i.e., it is a linear array), so locating spots is straightforward and requires computational time that scales linearly with the number of pixels in the array. In comparison, two-dimensional systems (e.g., camera images) have an additional search direction and increased area between spots, which require significantly more complex algorithms that demand computational time on the order of the square of the number of pixels (i.e., a factor of $10^2$−$10^3$ increase in computation time for typical sensor arrays).[50]

## ■ CONCLUSION

In summary, a powerful, inexpensive portable scanner has been developed for colorimetric array analysis that makes use of a novel line imager, the color contact image sensor (CIS). The device is superior to other common imaging methods in signal-to-noise and scan rate. The resulting scanner is small and lightweight; it is approximately the same size as a typical smartphone (albeit slightly thicker). The device is generalizable to any method that primarily uses colorimetry, including analysis of both gas- and liquid-phase analytes. Further miniaturization of this hand-held reader is also possible and relatively straightforward: the majority of its bulk comes from its battery and electronic elements. Additional development of CIS-based readers might increase the resolution of the optical imaging and could increase the number and range of


DOI: 10.1021/acs.analchem.5b01499
Anal. Chem. 2015, 87, 7810−7816

illumination sources, e.g., for hyperspectral imaging or fluorimetry.

## ■ ASSOCIATED CONTENT

### Supporting Information

Description of spot-finder algorithm and additional characterization of the hand-held unit. The Supporting Information is available free of charge on the ACS Publications website at DOI: 10.1021/acs.analchem.5b01499.

## ■ AUTHOR INFORMATION


### Corresponding Author

*E-mail: ksuslick@illinois.edu.


### Notes

The authors declare no competing financial interest.

## ■ ACKNOWLEDGMENTS

This work was supported by the U.S. NSF (CHE-1152232) and the U.S. Department of Defense (CTTSO/JIEDDO CB3614). Financial support by CTTSO/JIEDDO does not constitute an express or implied endorsement of the results or conclusions of the project by either CTTSO/JIEDDO or the U.S. Department of Defense.

## ■ REFERENCES


(1) Askim, J. R.; Mahmoudi, M.; Suslick, K. S. *Chem. Soc. Rev.* **2013**, *42*, 8649.
(2) McDonagh, C.; Burke, C. S.; MacCraith, B. D. *Chem. Rev.* **2008**, *108*, 400.
(3) Stewart, S.; Ivy, M. A.; Anslyn, E. V. *Chem. Soc. Rev.* **2014**, *43*, 70.
(4) Diehl, K. L.; Anslyn, E. V. *Chem. Soc. Rev.* **2013**, *42*, 8596.
(5) Lu, Y. X. *Prog. Chem.* **2014**, *26*, 931.
(6) Lim, S. H.; Feng, L.; Kemling, J. W.; Musto, C. J.; Suslick, K. S. *Nat. Chem.* **2009**, *1*, 562.
(7) Feng, L.; Musto, C. J.; Kemling, J. W.; Lim, S. H.; Suslick, K. S. *Chem. Commun.* **2010**, *46*, 2037.
(8) Feng, L.; Musto, C. J.; Kemling, J. W.; Lim, S. H.; Zhong, W.; Suslick, K. S. *Anal. Chem.* **2010**, *82*, 9433.
(9) Lin, H.; Suslick, K. S. *J. Am. Chem. Soc.* **2010**, *132*, 15519.
(10) Zhang, C.; Bailey, D. P.; Suslick, K. S. *J. Agric. Food Chem.* **2006**, *54*, 4925.
(11) Zhang, C.; Suslick, K. S. *J. Agric. Food Chem.* **2007**, *55*, 237.
(12) Suslick, B. A.; Feng, L.; Suslick, K. S. *Anal. Chem.* **2010**, *82*, 2067.
(13) Chen, Q. S.; Hui, Z.; Zhao, J. W.; Ouyang, Q. *Lwt-Food Science and Technology* **2014**, *57*, 502.
(14) Huang, X. W.; Zou, X. B.; Shi, J. Y.; Guo, Y. N.; Zhao, J. W.; Zhang, J. C.; Hao, L. M. *Food Chem.* **2014**, *145*, 549.
(15) Li, H. H.; Chen, Q. S.; Zhao, J. W.; Ouyang, Q. *Anal. Methods* **2014**, *6*, 6271.
(16) Li, J. J.; Song, C. X.; Hou, C. J.; Huo, D. Q.; Shen, C. H.; Luo, X. G.; Yang, M.; Fa, H. B. *J. Agric. Food Chem.* **2014**, *62*, 10422.
(17) Zaragoza, P.; Ros-Lis, J. V.; Vivancos, J. L.; Martinez-Manez, R. *Food Chem.* **2015**, *172*, 823.
(18) Shetty, V.; Zigler, C.; Robles, T. F.; Elashoff, D.; Yamaguchi, M. *Psychoneuroendocrinology* **2011**, *36*, 193.
(19) Martinez-Olmos, A.; Capel-Cuevas, S.; Lopez-Ruiz, N.; Palma, A. J.; de Orbe, I.; Capitan-Vallvey, L. F. *Sens. Actuators, B* **2011**, *156*, 840.
(20) Carey, J. R.; Suslick, K. S.; Hulkower, K. I.; Imlay, J. A.; Imlay, K. R. C.; Ingison, C. K.; Ponder, J. B.; Sen, A.; Wittrig, A. E. *J. Am. Chem. Soc.* **2011**, *133*, 7571.
(21) Lonsdale, C. L.; Taba, B.; Queralto, N.; Lukaszewski, R. A.; Martino, R. A.; Rhodes, P. A.; Lim, S. H. *PLoS One* **2013**, *8*, e62726.
(22) Chen, Q. S.; Li, H. H.; Ouyang, Q.; Zhao, J. W. *Sens. Actuators, B* **2014**, *205*, 1.
(23) Zaragoza, P.; Fernandez-Segovia, I.; Fuentes, A.; Vivancos, J. L.; Ros-Lis, J. V.; Barat, J. M.; Martinez-Manez, R. *Sens. Actuators, B* **2014**, *195*, 478.
(24) Ohta, J. *Smart CMOS Image Sensors and Applications*; CRC Press: Boca Raton, FL, 2007.
(25) CMOS Sensor Inc. 300−600 DPI Contact Image Sensor. http://www.csensor.com/M116_CIS.htm (accessed Jan 28, 2014).
(26) Schwarzer Precision. 100 EC-LC Eccentric Diaphragm Pumps. http://www.schwarzer.com/pages_en/produkt.php?id=191 (accessed Jan 31, 2014).
(27) Rakow, N. A.; Suslick, K. S. *Nature* **2000**, *406*, 710.
(28) Suslick, K. S. *MRS Bull.* **2004**, *29*, 720.
(29) Suslick, K. S.; Rakow, N. A.; Sen, A. *Tetrahedron* **2004**, *60*, 11133.
(30) Janzen, M. C.; Ponder, J. B.; Bailey, D. P.; Ingison, C. K.; Suslick, K. S. *Anal. Chem.* **2006**, *78*, 3591.
(31) Sen, A.; Albarella, J. D.; Carey, J. R.; Kim, P.; McNamara Iii, W. B. *Sens. Actuators, B* **2008**, *134*, 234.
(32) Lin, H.; Jang, M.; Suslick, K. S. *J. Am. Chem. Soc.* **2011**, *133*, 16786.
(33) Kolthoff, I. M. *Acid−Base Indicators*; Macmillan: New York, 1937.
(34) Petersen, J.; Stangegaard, M.; Birgens, H.; Dufva, M. *Anal. Biochem.* **2007**, *360*, 169.
(35) Walt, D. R. *BioTechniques* **2006**, *41*, 529.
(36) Steiner, M.-S.; Meier, R. J.; Duerkop, A.; Wolfbeis, O. S. *Anal. Chem.* **2010**, *82*, 8402.
(37) García, A.; Erenas, M. M.; Marinetto, E. D.; Abad, C. A.; de Orbe-Paya, I.; Palma, A. J.; Capitán-Vallvey, L. F. *Sens. Actuators, B* **2011**, *156*, 350.
(38) Lapresta-Fernandez, A.; Capitan-Vallvey, L. F. *Analyst* **2011**, *136*, 3917.
(39) Lapresta-Fernández, A.; Capitán-Vallvey, L. F. *Anal. Chim. Acta* **2011**, *706*, 328.
(40) Dini, F.; Filippini, D.; Paolesse, R.; Lundström, I.; Di Natale, C. *Sens. Actuators, B* **2013**, *179*, 46.
(41) Iqbal, Z.; Eriksson, M. *Sens. Actuators, B* **2013**, *185*, 354.
(42) Vallejos, S.; Munoz, A.; Ibeas, S.; Serna, F.; Garcia, F. C.; Garcia, J. M. *J. Mater. Chem. A* **2013**, *1*, 15435.
(43) Martinez, A. W.; Phillips, S. T.; Whitesides, G. M.; Carrilho, E. *Anal. Chem.* **2010**, *82*, 3.
(44) Iqbal, Z.; Bjorklund, R. B. *Talanta* **2011**, *84*, 1118.
(45) Shen, L.; Hagen, J. A.; Papautsky, I. *Lab Chip* **2012**, *12*, 4240.
(46) Oncescu, V.; O'Dell, D.; Erickson, D. *Lab Chip* **2013**, *13*, 3232.
(47) Wei, Q.; Nagi, R.; Sadeghi, K.; Feng, S.; Yan, E.; Ki, S. J.; Caire, R.; Tseng, D.; Ozcan, A. *ACS Nano* **2014**, *8*, 1121.
(48) Ellerbee, A. K.; Phillips, S. T.; Siegel, A. C.; Mirica, K. A.; Martinez, A. W.; Striehl, P.; Jain, N.; Prentiss, M.; Whitesides, G. M. *Anal. Chem.* **2009**, *81*, 8447.
(49) Lee, D.-S.; Jeon, B. G.; Ihm, C.; Park, J.-K.; Jung, M. Y. *Lab Chip* **2011**, *11*, 120.
(50) Flach, P. *Machine Learning: The Art and Science of Algorithms that Make Sense of Data*; Cambridge University Press: Cambridge, U.K., 2012.




DOI: 10.1021/acs.analchem.5b01499
*Anal. Chem.* 2015, 87, 7810−7816